Chromosome Research **8**: 571–584, 2000.

Organization of the X and Y chromosomes in human, chimpanzee and mouse pachytene nuclei using molecular cytogenetics and three-dimensional confocal analyses

C. Metzler-Guillemain[1,2], Y. Usson[3], C. Mignon[1], D. Depetris[1], G. Dubreuil[4], M. R. Guichaoua[2] & M. G. Mattei[1]*

[1] *Inserm U491, Faculté de Médecine Timone, 27, Bd Jean Moulin, 13385 Marseille cedex 05, France; Tel: (33) 04 91 25 71 73; Fax: (33) 04 91 80 43 19; E-mail: genevieve.mattei@medecine.univ-mrs.fr;* [2] *Laboratoire de Biologie de la Reproduction et du Développement, Faculté de Médecine Nord, Bd Pierre Dramard, 13326 Marseille cedex 15, France;* [3] *TIMC UMR 5525 CNRS, Institut Albert Bonniot, Université Joseph Fourier-Grenoble 1, La Tronche, France;* [4] *Centre International de Recherches Médicales, Franceville, Gabon*

* *Correspondence*

Received 24 March 2000; received in revised form and accepted for publication by B. Dutrillaux 26 May 2000

Key words: chimpanzee, chromatin condensation, human, mouse, XY body

Abstract

We used multicolour fluorescence *in-situ* hybridization on air-dried pachytene nuclei to analyse the structural and functional domains of the sex vesicle (SV) in human, chimpanzee and mouse. The same technology associated with 3-dimensional analysis was then performed on human and mouse pachytene nuclei from cytospin preparations and tissue cryosections. The human and the chimpanzee SVs were very similar, with a consistently small size and a high degree of condensation. The mouse SV was most often seen to be large and poorly condensed, although it did undergo progressive condensation during pachynema. These results suggest that the condensation of the sex chromosomes is not a prerequisite for the formation of the mouse SV, and that a different specific mechanism could be responsible for its formation. We also found that the X and Y chromosomes are organized into two separate and non-entangled chromatin domains in the SV of the three species. In each species, telomeres of the X and Y chromosomes remain clustered in a small area of the SV, even those without a pseudoautosomal region. The possible mechanisms involved in the organization of the sex chromosomes and in SV formation are discussed.

Introduction

During pachynema in male mammals, the X and Y chromosomes form a nuclear structure attached to the nuclear membrane. This structure is known as the XY body or sex vesicle (SV). Unlike the autosomal bivalents, the XY body is characterized by a particular chromatin condensation and transcriptional inactivation (Solari 1974, 1989). It has been hypothesized that the differential

chromatin condensation of sex chromosomes during meiotic prophase renders the DNA inaccessible not only to transcriptases but also to recombinases (McKee & Handel 1993), and thus serves to prevent deleterious crossing over between non-homologous regions of the X and Y chromosomes. Within the sex vesicle, the X and Y chromosomes are paired by their pseudo-autosomal regions and the progressive entanglement of their unpaired axes has been described from spread preparations (Solari 1980, Chandley *et al*. 1984). Nevertheless, little is known about the organization of the X and Y chromosomes in the SV or the factors that play a role in their condensation. It has been suggested that SV condensation depends on the action of specific factors, which may include the XIST/Xist transcript (Richler et al. 1992, Ayoub et al. 1997), some specific proteins (Parraga & Del Mazo 2000), or the heterochromatin content of the sex chromosomes. Using molecular cytogenetics and conventional microscopy (2D-analysis), we analysed the structural and functional domains of the SV in human, chimpanzee and mouse. Confocal scanning microscopy was subsequently performed in conjunction with three-dimensional (3D) reconstruction of human and mouse SVs. In the three species studied, the sex chromosomes differ in terms of morphology, heterochromatin content and sequence homology, factors possibly involved in the organization or the condensation of the SV.

Materials and methods

Testicular material was obtained from human, chimpanzee and mouse individuals, all having a normal karyotype.

Human testicular samples and slide preparation

Human testicular material was obtained from two men who underwent orchidectomy in the management of prostate carcinoma. The testes were cut into small fragments (0.5 cm^3) and treated by three different protocols.

Protocol 1: Air dried preparations

Testicular samples were immediately fixed in 3 : 1 methanol/ acetic acid to obtain air-dried preparations as described by Luciani *et al*. (1975). Slides were stored at −80°C.

Protocol 2: Cytospin preparations

In order to obtain meiotic spreads for analysis of 3D structure, other testicular samples were teased with forceps in HAM-F10 medium to obtain a cell suspension. After centrifugation, the supernatant was removed and the pellet resuspended in HAM-F10 medium containing 10% glycerol. This suspension was distributed in aliquots and stored in liquid nitrogen (−196°C) until use. After thawing, cells were cytocentrifuged on silane-coated slides (200 rpm for 5 min in a Cytospin 2 Shandon). Cytocentrifuged preparations were fixed in PBS containing 4% paraformaldehyde for 10 min and rinsed in PBS before *in situ* hybridization.

Protocol 3: Tissue cryosections

Entire testicular fragments were gently frozen in liquid nitrogen, stored at −196°C and subsequently cryosectioned. Cryosections, 10–12μm thick, were laid on silane-coated slides (Sigma), fixed in PBS containing 4% paraformaldehyde for 30 min, rinsed 3 times in PBS, dehydrated and stored at −196°C prior to use. After thawing and rehydratation in PBS, sections were permeabilized with PBS containing 0.5% Triton X-100 for 35 min, rinsed in PBS and digested with trypsin, 0.2 mg/ml, in PBS under a coverslip at 37°C for 40 min. Slides were then rinsed in PBS, fixed in PBS containing 4% paraformaldehyde for 10 min, rinsed once more in PBS, ethanol dehydrated and dried prior to processing for hybridization.

Chimpanzee testicular samples and slide preparation

A testicular biopsy made under general anaesthesia was obtained from a healthy male chimpanzee (*Pan troglodytes*) from the CIRM (Centre International de Recherches Médicales, Franceville, Gabon), after approval from the CECUA (Centre d'Étude et de Contrôle de l'Usage des Animaux). Only air-dried pre-

parations without KCl hypotonic treatment (protocol 1) were made from the chimpanzee testicular biopsy.

Mouse testicular samples and slide preparation

Meiotic preparations from two C57BL6 mice and three WMP mice (gift from J. L. Guénet; Bonhomme & Guénet, 1989) were obtained by the same three protocols as those used with human samples.

Probes and labelling

The different probes used to study the human, chimpanzee and mouse sex vesicles are summarized in Table 1. The human YAC clones, 946f5 and 957f8, obtained from the CEPH (Centre d'Étude du Polymorphisme Humain), were amplified using Alu-PCR (Lengauer *et al.* 1992). PCR products were labelled with biotine 14-dCTP by random priming (Bioprime DNA labeling system, Life Technologies) before hybridization. The mouse PA-2 YAC (kindly provided by E. Heard) was amplified by PCR of B1 sequences with the primer 5′ GCA CAC GCC TTT AAT CCC AGC 3′ (Rettenberger *et al.* 1995). The PA-2 PCR products and the P68 probe (kindly provided by C. Vourc'h) were labelled with biotin 14-dCTP or digoxigenin 11-dUTP (Dig-High Prime, Roche Diagnostics) by random priming, before hybridization on mouse meiotic cells. A synthetic peptide nucleic acid PNA-$(C_3TA_2)_3$ oligonucleotide probe (Lansdorp *et al.* 1996) was used for the detection of the telomeric TTAGGG repeats on human, chimpanzee and mouse spermatocytes.

Fluorescent in-situ *hybridization (FISH) experiments*

Air-dried preparations were thawed, treated and denatured as previously described (Metzler-Guillemain *et al.* 1999). In order to preserve the 3D-structure of nuclei, cytospin preparations and cryosections were denatured on a plate between 75°C and 80°C for 5 min. Commercial DNA probes were hybridized and the signal detected as recommended by the manufacturers. All probes were first hybridized on somatic metaphase chromosomes in order to establish the hybridization parameters.

Human and mouse YAC probes were used at 300 ng/slide after a competition with 90 μg of human or mouse Cot-I DNA (Roche Diagnostics and Life Technologies, respectively). The mouse P68 probe was used at 20 ng/slide without competition. Detection was performed as previously described (Pinkel *et al.* 1986). Hybridization and detection of the Cy3 PNA-telomeric probe was performed on air dried meiotic preparations as described for somatic cells (Lansdorp *et al.* 1996). Preparations were counterstained either with 4,6-diamidino 2-phenyl indole (DAPI) at 100 ng/ml in Vectashield mounting media (Vector Laboratories), or with TO-PRO 3 (Molecular Probes) at a 1 : 100 dilution in Vectashield for confocal analysis.

Light-microscopic analysis

Pachytene nuclei were observed using an Axioplan-2 Zeiss fluorescent microscope. The images were captured with a CCD camera (photometrics 'SenSys'). Information was collected and merged using IPLab Spectrum software (Vysis). At least 100 SVs from air-dried preparations were analysed for each combination of probes in each species. Some X and Y paint probe signals in pachytene nuclei were also captured from mouse and human cytospin spreads and testis cryosections, in order to evaluate the size of the SV in these preparations.

Confocal analysis and 3D-reconstruction

Confocal microscopy followed by 3D analysis was performed on pachytene nuclei from protocols 2 and 3 of human and mouse. Thirty nuclei from cytospin preparations (protocol 2) were analysed in order to determine the 3D structure of the X and Y chromosomes in the sex vesicle and the nuclear volume. The 3D parameters of the sex chromosomes were also determined in thirty nuclei from testis cryosections (protocol 3), in order to avoid bias due to tissue disaggregation or freeze-thawing of the preparations.

Table 1. Characteristics of the probes used on human, chimpanzee and mouse meiotic preparations.

Probe number	Probes used	Location	Reference	Provider
	On human and chimpanzee meioses			
	X probes			
1a	Human X paint	Whole X chromosome	WCP X spectrum orange	Vysis
1b	Human X paint	Whole X chromosome	WCP X spectrum green	Vysis
2	Human XIST DNA	Xq13.3	P5122-DG.5	Oncor
3a	Human DXZ1 α-satellite	X centromere	P5060-B.5	Oncor
3b	Human DXZ1 α-satellite	X centromere	P5060-DG.5	Oncor
4	YAC Xp	Xp21	946f5	CEPH
5	YAC Xq	Xq25	957f8	CEPH
	Y probes			
6a	Human Y paint	Whole Y chromosome	WCP Y spectrum green	Vysis
6b	Human Y paint	Whole Y chromosome	WCP Y spectrum orange	Vysis
7	Human DYZ1 satellite	Yq11	P5061-B.5	Oncor
8	Human chromosome Y cocktail	Y centromere + Yq11	P5062-DG.5	Oncor
	On mouse meiosis			
9a	Mouse X paint probe	whole X chromosome	P6120-DG.5	Oncor
9b	Mouse X paint probe	whole X chromosome	1189-XMF	Cambio
10a	Mouse Y paint probe	whole Y chromosome	P6121-B.5	Oncor
10b	Mouse Y paint probe	whole Y chromosome	1200-YMCy3	Cambio
11	YAC PA-2	XD, Xist locus	Heard *et al.* 1999	P. Avner
12	P 68	XA, subcentromeric	Disteche *et al.* 1985	C. Vourc'h
	On human, chimpanzee and mouse meioses			
13	PNA oligonucleotide $(C_3TA_2)_3$ probe	All telomeres	Lansdorp *et al.* 1996	Perseptive Biosystems

Optical settings
Series of confocal optical sections were obtained using a Zeiss LSM410 confocal microscope equipped with three laser sources and three confocal detectors. The images of the confocal sections were collected with a 63× NA 1.3 Planapochromat objective lens. One optical section was recorded every 200 nm along the z axis and the pixel sampling was 100 nm along the x and y axes.

3D image analysis
The confocal series were visualized and processed with the Edit3D and Ana3D programmes (Parazza *et al*. 1993, 1995). In brief, Edit3D was used to generate 3D reconstructions of the data sets and Ana3D was used to extract morphological features according to the following procedure. For each channel, the histogram of fluorescence intensities was stretched in order to fill the full dynamic range of eight bit images. Then, an adaptive low-pass filter was applied to each channel in order to remove photonic noise from the images. The binary masks of nucleus, X chromosome and Y chromosome were obtained by applying a fixed intensity threshold to the data set. A 3D labelling algorithm was used to filter out small objects corresponding to non-specific labelling and extract the volumes to be measured.

Results

FISH with various probes allowed the specific chromatin domains of the X and Y chromosomes to be unequivocally identified in the sex vesicle.

Condensation and organization of the human sex vesicle

2D analysis
In human male pachytene nuclei, the SV appeared as a small, rounded, substructure showing a high degree of condensation in all substages. Co-hybridization of differently labelled X and Y paint probes to air-dried preparations of pachytene nuclei (probe combination 1a+6a; Table 1), showed two juxtaposed fluorescent signals without intermingling or superposition of the corresponding chromosomal domains (Figure 1A). This observation was confirmed on cytospin preparations and tissue cryosections. The X centromere alphoid probe was co-hybridized with the probe specific for the Yq11 heterochromatic region (probe combination 3b + 7) and revealed diametrically opposite signals in the human SV, suggesting that the X and Y are organized into two completely separate chromosomal domains. The XIST probe hybridized with the X centromere probe showed two signals located in the same peripheral area of the SV, diametrically opposite to the Y heterochromatin domain (probe combination 2 + 3a + 7 + 8) (Figures 1B and B*). Simultaneous hybridization of two YAC probes from the X chromosome, 957f8 (Xp21.3) and 946f5 (Xq26-q27), with the X centromere probe (probe combination 3b + 4 + 5) showed that both YAC signals were located in the same central area of the sex vesicle (Figure 1C). This result indicates that the two arms of the X chromosome are brought together in the SV, with the X centromere located at the folding point of this chromosome. Hybridization with the PNA-$(C_3TA_2)_3$ probe showed that all X and Y telomere signals were clustered in the same peripheral area of the SV in all pachytene nuclei. Moreover, in 90% of these nuclei, only two juxtaposed signals were detectable, suggesting a two-by-two telomeric association (Figure 1D).

3D analysis
3D reconstruction of pachytene nuclei hybridized with X and Y paint probes (combination 1b + 6b) confirmed the juxtaposition of independent and well-defined X and Y chromosome domains in the SV (Figure 2A). The 3D parameters analysed are reported in Table 2. As expected, the mean value of the human X chromosome volume was larger than the mean value of the Y chromosome volume in both cytospin preparations and tissue cryosections. Although the X and Y chromosome volumes were larger in cytospin preparations than in cryosections, the vX/vY ratios were similar in both types of preparation. The volume of pachytene nuclei (vN) was only determined on cytospin preparations, where nuclei are fully available. The organization of the X

and Y chromosome domains in the human SV, based on both the 2D and 3D-analyses, is schematically represented in Figure 2B.

Condensation and organization of the chimpanzee sex vesicle

The chimpanzee SV from air-dried preparations appeared very similar to that of human, except for the absence of a strongly DAPI-stained region corresponding to the human Y chromosome heterochromatic material. Co-hybridization of X and Y paint probes (probe combination 1a + 6a) gave two distinct fluorescent areas (Figure 3A), as in human. The chimpanzee SV organization was shown to be similar to the human one, with both the following combinations: the XIST and X centromere probes (combination 2+3a); the YAC 957f8, YAC 946f5 and the X centromere probes (combination 3b + 4 + 5). Hybridization of the PNA-$(C_3TA_2)_3$ telomeric sequences gave the same results as in human, with most often two signals detected in the SV (Figure 3B).

Condensation and organization of the mouse sex vesicle

2D analysis

The mouse SV appeared very different from the human and chimpanzee SVs on air-dried preparations. At early pachynena, the mouse SV appeared as a large pear, poorly condensed, located far from the autosomal bivalents. In late pachytene nuclei, the mouse SV appeared smaller and more condensed.

FISH experiments on air-dried preparations with murine X and Y paint probes (probe combination 9a + 10a) confirmed the large size of the SV and suggested that it consisted of two separate chromosomal domains placed one above the other (Figure 3C). Hybridization of the p68 probe, known to be adjacent to the X centromere heterochromatin on metaphase chromosomes (Disteche *et al*. 1985), gave a signal located far from the X centromere in all SVs observed, even in the more compact ones. This suggested that the proximal region of the X chromosome is part of a domain which is maintained in a highly decondensed state within the SV. Cohybridization of p68 and YAC PA-2 containing the mouse Xist gene (probe combination 11 + 12) showed two signals in the same area of the SV (Figure 3D). Taking into account the distance between the corresponding loci on the X metaphase chromosome and the undercondensation of the X chromosome in the SV, this observation suggests that the X chromosome is formed into at least two loops in the mouse SV. The PNA-$(C_3TA_2)_3$ telomere probe signals revealed that all four telomeric ends form a cluster in nearly all the SVs (Figure 3E).

3D analysis

Confocal serial sectioning of pachytene nuclei on mouse cytospin preparations and testis sections hybridized with X and Y paint probes (combination 9b + 10b) confirmed the preponderance of large SVs and their organization in two separate domains. Quantitative 3D analysis revealed that the X chromosome domain occupies a larger volume than the Y chromosome domain, both on cytospin preparations and on tissue cryosections (Table 3, Figure 2D). The SV volume (vSV = vX + vY) had a mean value of 60.1 μm^3 in cytospin preparations and 40.4 μm^3 in cryosections (Table 3). In contrast to the human

Figure 1 (opposite). Organization of the X and Y chromosomes in human pachytene nuclei from air dried preparations counterstained with DAPI. (**A**) Details of four sex vesicles (SV) showing two separate X and Y chromosome domains visualized with X (red signal) and Y (green signal) paint probes. (**B & B***) Three partial pachytene nuclei showing the relative position of the X and Y chromosomes in the SV: X centromere (green signal), XIST locus (isolated red signal), Y centromere (red signal close to the yellow one) and Yq11 heterochromatic region (yellow signal). The yellow Yq11 signal results from hybridization of an equal mix of biotin-labelled DYZ1 and digoxigenin-labelled DYZ1 probes. (**C**) Details of two SVs showing the folding of the X chromosome, its centromere being located at the folding point: X centromere (red signal), YACs 957f8 located at Xp21.3 and 946f5 located at Xq26-q27 (green signals). (**D**) Four partial pachytene nuclei hybridized with the PNA-$(C_3TA_2)_3$ probe which allows the detection of all telomeres (red signals): in the SVs, only one or two juxtaposed signals are detectable, suggesting that the X and Y telomeres are associated two by two. Scale bar = 10 μm

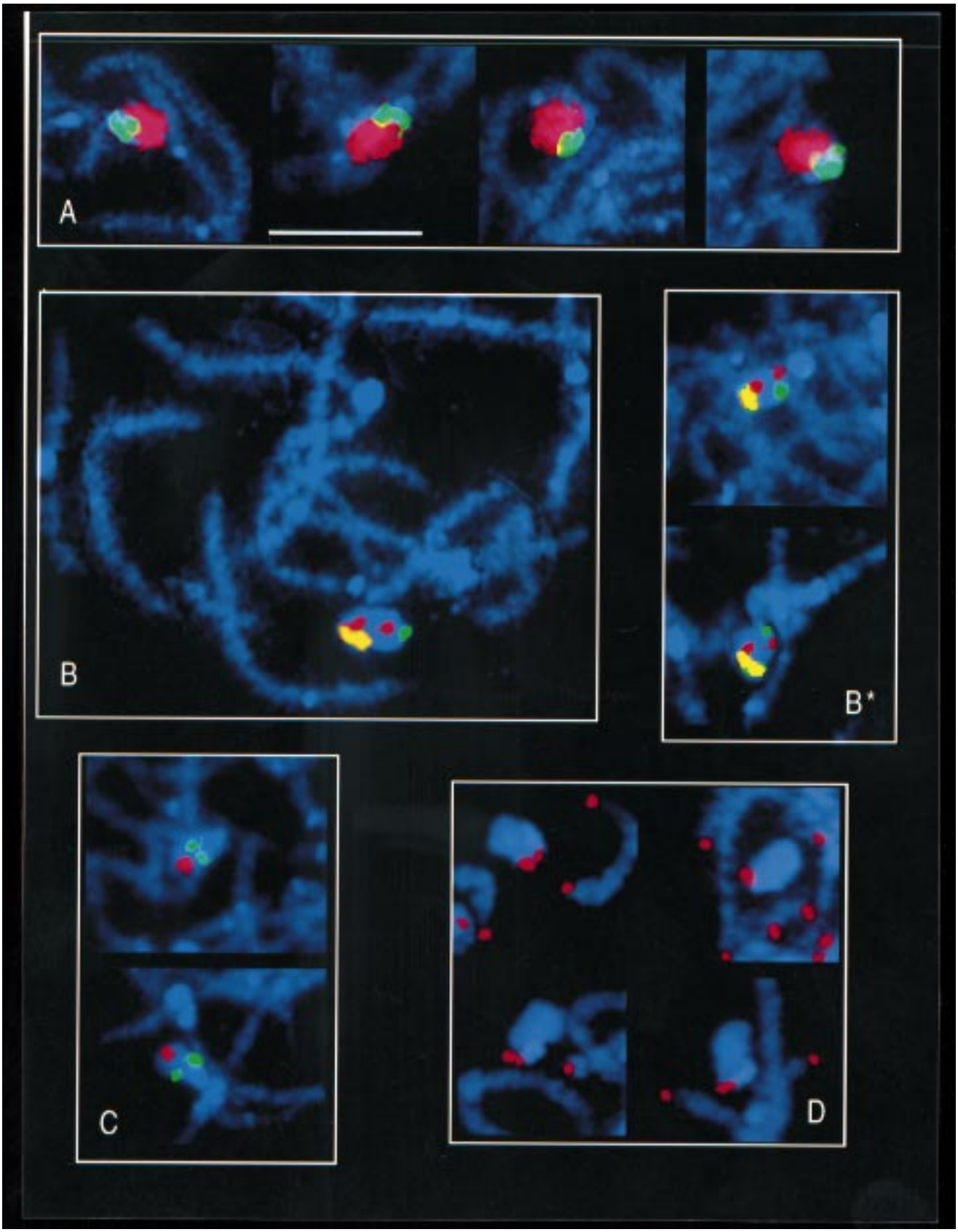
A
B
B*
C
D

Table 2. Mean values (ISD) of the 3D parameters analysed in human pachytene nuclei.

	X volume vX (μm^3)	Y volume vY (μm^3)	SV volume vSV = vX + vY (μm^3)	Nucleus volume vN (μm^3)	vX/vY (%)	vSV/vN (%)
Cytospin preparations	33.26 (±10.2)	12.63 (±5.43)	45.9 (±14.6)	1257.8 (±300.8)	2.63 (±1.13)	3.6 (±1.22)
Cryosections	21.73 (±6.26)	7.08 (±1.05)	28.8 (±6.0)	—	3.06 (±1.38)	—

situation, the vX/vY ratio in mouse cytospin preparations was much lower than that observed in mouse cryosections (Table 3). The mean value of the nucleus volume was only determined on cytospin preparations, where nuclei are complete (Table 3).

A schematic representation of the proposed organization of the X and Y chromosomes in the mouse SV is shown in Figure 2C.

Discussion

Comparative 2D and 3D analyses of human, chimpanzee and mouse

Our 2D-studies have demonstrated that human and chimpanzee SVs are very similar, except that no prominent heterochromatin domain was detectable in the chimpanzee SV. This is in agreement with the observation that the chimpanzee Y chromosome only contains a small heterochromatic region located on its short arm (Schnedl *et al*. 1975, Schmid & Haaf 1984). Both SVs appear as small ovoid structures, which are pycnotic and remain highly condensed throughout pachynema in all types of preparation. In sharp contrast, the mouse SV is in the form of a large undercondensed pear, isolated from the autosomal bivalents in the majority of pachytene nuclei. Our comparative 3D-studies confirmed these differences, with the volume of the mouse SV being significantly larger than that of the human ($p < 0.01$ and $p < 0.001$ on cytospin preparations and cryosections, respectively). Moreover, the mouse SV volume is certainly underestimated as it does not include the large heterochromatic X-centromere region, which is not labelled by the X paint probe. Two points are, nevertheless, worthy of note. Firstly, the X and Y average volumes are larger on cytospin preparations than on cryosections, both in human and mouse pachytene nuclei. This may result from a greater flattening of nuclei or some chromatin unwinding, due to the centrifugation applied to cytospin material. Secondly, in mouse, the vX/vY ratio on cytospin preparations is lower than that determined on cryosections, in contrast to the corresponding ratios in human (Tables 2 and 3). The undercondensation of the mouse X chromosome, responsible for its usual faint signal, might be increased by the cytospin protocol, leading to an underestimation of the corresponding volume (vX). Nevertheless, the mouse SV is on average larger than the human one, either in terms of absolute value, or its volume relative to the nucleus volume.

Organization of the X and Y chromosomes in human, chimpanzee and mouse sex vesicles

Our FISH experiments with different probes on all types of nuclear preparation demonstrate that the X and Y chromosomes form two separate domains

Figure 2 (opposite). Three-dimensional reconstruction of human and mouse sex vesicles (SV). (**A**) Human SV: four selected views from the same SV showing the spatial arrangement of the X (green signal) and Y (red signal) chromosomes. (**B**) Schematic representation of the human SV: the X (blue) and Y (dark) chromosomes are attached to the nuclear membrane (grey) by their telomeres (red). (**C**) Schematic representation of the mouse SV: the X (blue) and Y (dark) chromosomes are attached to the nuclear membrane (grey) by their telomeres (red). (**D**) Mouse SV: four selected views from the same SV showing the spatial arrangement of the X (green signal) and Y (red signal) chromosomes. Scale bar = 5 μm.

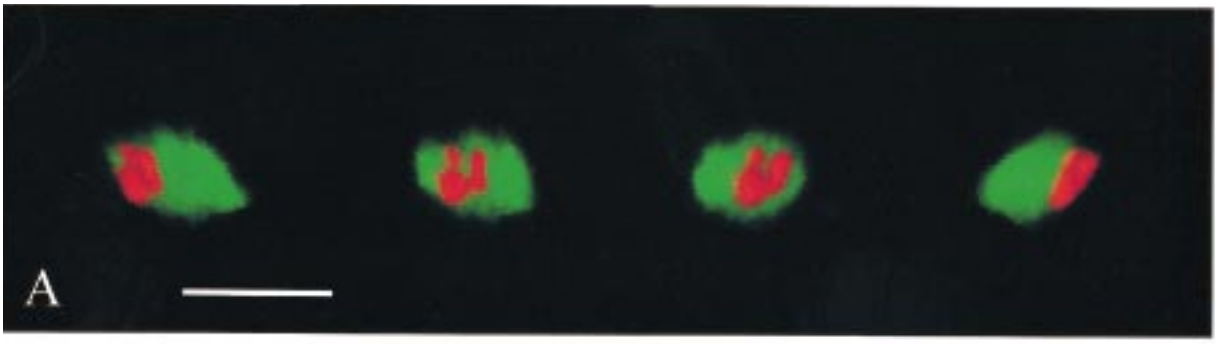
A

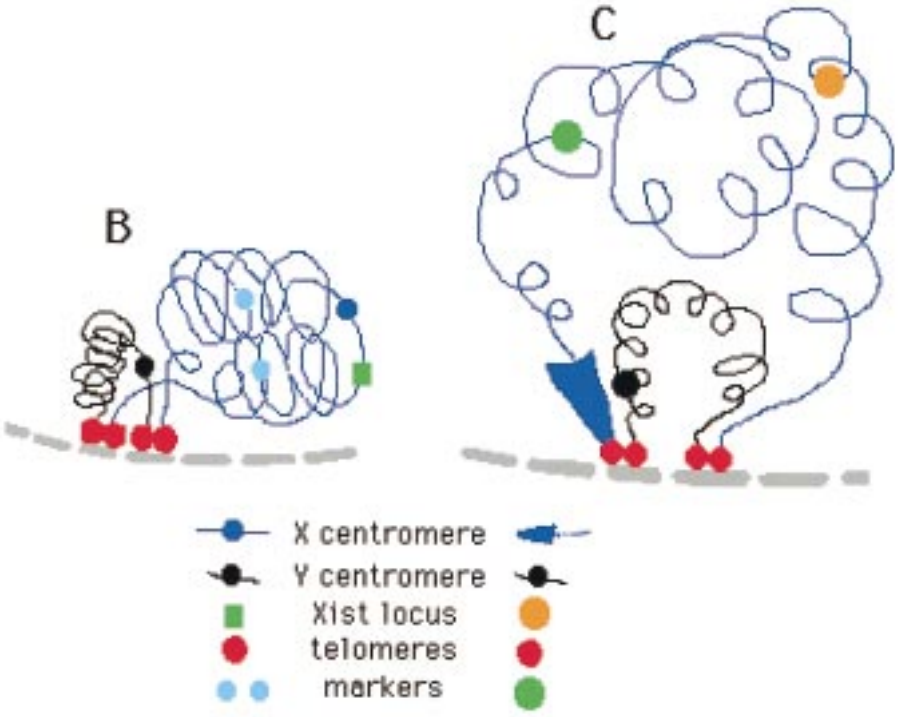
B
C
X centromere
Y centromere
Xist locus
telomeres
markers

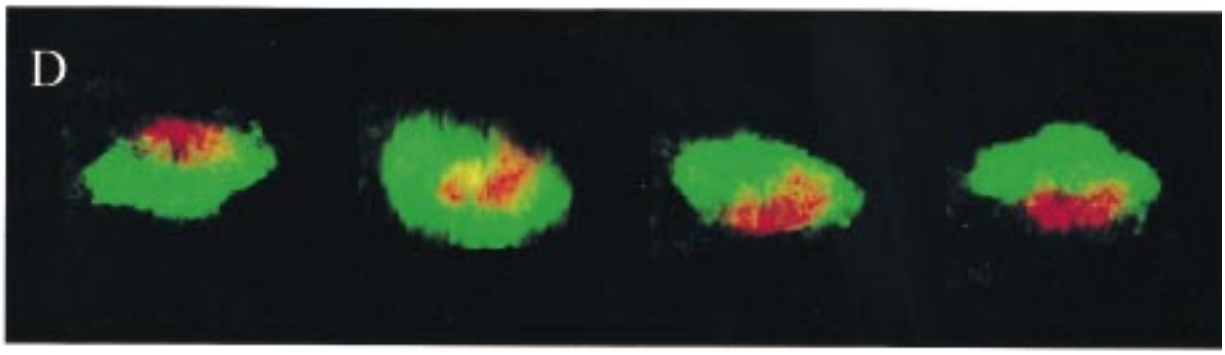
D

Table 3. Mean values (ISD) of the 3D-parameters analysed in mouse pachytene nuclei.

	X volume vX (μm^3)	Y volume vY (μm^3)	SV volume vSV = vX + vY (μm^3)	Nucleus volume vN (μm^3)	vX/vY (%)	vSV/vN (%)
Cytospin preparations	38.23 (±14.9)	21.89 (±6.34)	60.1 (±18.9)	941.8 (±334.9)	1.74 (±1.14)	6.3 (±1.18)
Cryosections	28.71 (±7.83)	11.72 (±4.76)	40.4 (±10.5)	—	2.44 (±1.61)	—

in the SV of human, chimpanzee and mouse. These results differ from previous reports describing an entangled packing of the X and Y axes in the SV (Solari 1980, Chandley *et al*. 1984), but are in agreement with the observation that the X centromere and the Y heterochromatin are situated at opposite poles of the human SV (Armstrong *et al*. 1994). Both the morphology and the chromatin organization of human and mouse SVs, deduced from 2D observations on air-dried preparations, were confirmed by 3D confocal analysis on cytospin preparations and tissue sections. The separate organization of their respective chromatin domains appears to be a simple way to prevent accidental recombination events between differentiated regions of the X and Y chromosomes. This result supports the hypothesis that nuclear organization of individual chromosome domains may be functionally important (Popp *et al*. 1990).

Despite the separation of the bulk of the X and Y chromatin in the SV of all three species, the X and Y chromosome domains do join their ends, as demonstrated by the clustering of their four telomeres. In humans, such an organization could be explained by the necessity for the two pseudoautosomal regions (PAR1 and PAR2) to reside in the same 'active' area of the SV. Nevertheless, only one pseudoautosomal region has been identified on the sex chromosomes of chimpanzee (Kvalov *et al*. 1994, Graves *et al*. 1998) and mouse (Burgoyne 1982, Salido *et al* 1998). Therefore, the lack of a second pseudoautosomal region on the X and Y chromosomes does not prevent them from bending together and joining their four telomeres. A similar aspecific end-joining of the sex chromosomes has been observed in the SV of several species of marsupials, which have no pseudoautosomal region on their sex chromosomes (Sharp 1982, Solari 1989, Graves *et al*. 1998). In these marsupial species, pairing is observed either between X and Y telomeres, or between telomeres from the same chromosome. These observations suggest that the telomere clustering observed in all types of SV does not reflect a particular role of the pseudoautosomal regions but may be a remnant of the 'bouquet' structure formed at zygonema. During zygonema and pachynema, all telomeres are thought to be attached to the inner surface of the nuclear envelope (Sherthan *et al*. 1996). As the pairing of homologous regions progresses, the telomeres from

Figure 3 (opposite). Oganization of the X and Y chromosomes in chimpanzee (**A, B**) and mouse (**C, D, E**) pachytene nuclei from air dried preparations. (**A**) Four chimpanzee sex vesicles (SV) showing two separate X (red signal) and Y (green signal) chromosome domains visualized with paint probes. The discrete yellow signal corresponds to the superposition of green and red signals. (**B**) Details of four chimpanzee pachytene nuclei hybridized with the PNA-$(C_3TA_2)_3$ probe which allows the detection of all telomeres (red signals): in the SVs, only one or two juxtaposed signals are detectable, suggesting that the X and Y telomeres are associated two by two. (**C**) Four isolated mouse sex vesicles (SV) showing the undercondensation of the X (red signal) and Y (geen signal) chromosomes and their separation into two distinct domains in the SV. The diffuse yellow signal corresponds to the superposition of the red and green signals. (**D**) Panel showing the folding of the X chromosome in four isolated mouse SVs: note that the P68 probe (green signal) is located far from the X centromeric heterochromatin (bright fluorescence with DAPI staining) and in the same domain as the PA-2 YAC probe (red signal). (**E**) Four isolated mouse SVs from pachytene nuclei hybridized with the PNA-$(C_3TA_2)_3$ probe. The four telomeres of the X and Y chromosomes are clustered in the same area of the SVs (telomeres=red signals). Scale bar = 5 μm

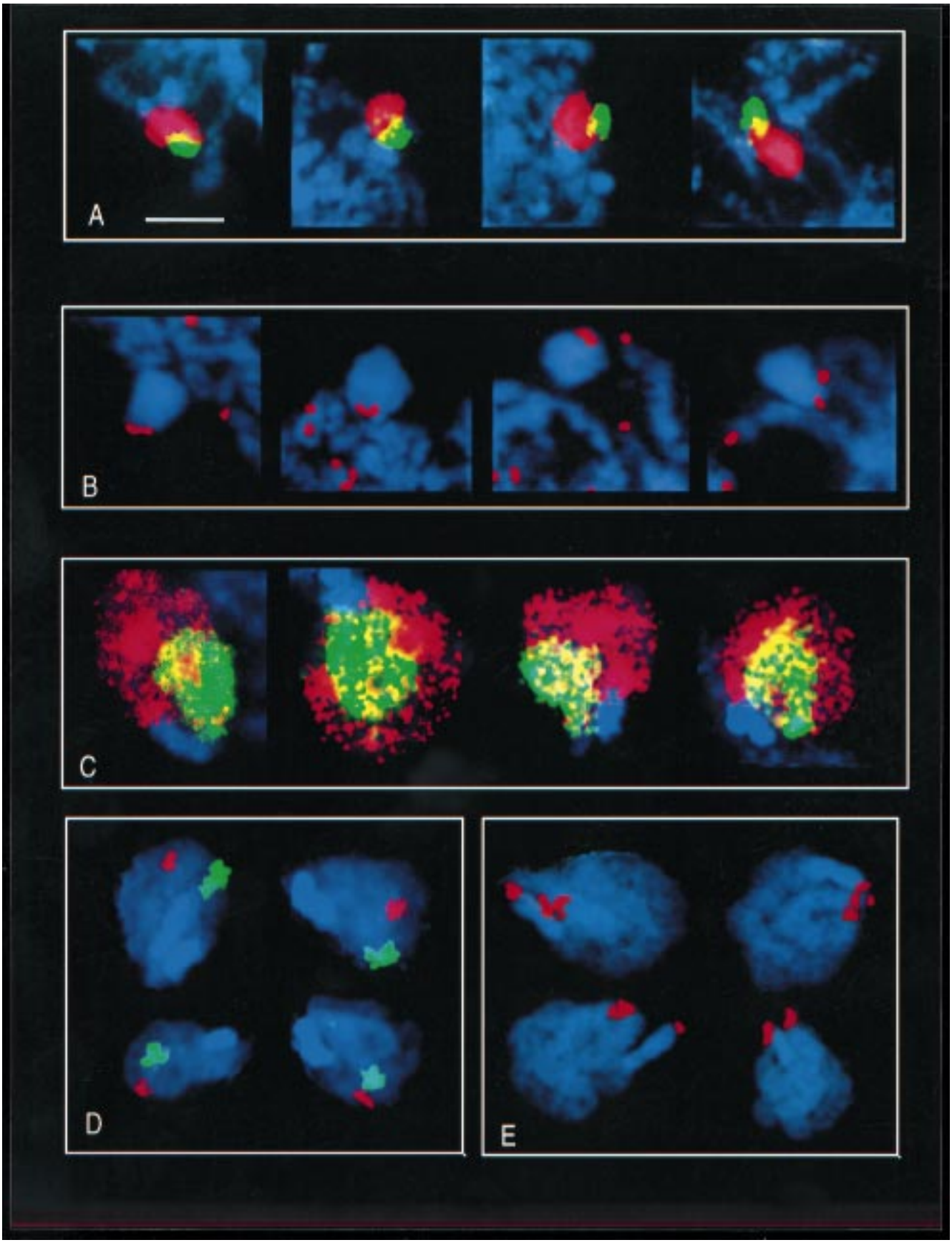
A
B
C
D
E

autosomal bivalents are dispersed by various pairing forces throughout the nuclear periphery. In contrast, in the absence of other pairing forces, the telomeres of the sexual bivalent may remain close together. This might be an important process for the initiation of the SV formation.

Condensation of the X and Y chromosomes in human, chimpanzee and mouse sex vesicles

The undercondensation of the mouse SV that we observed in 2D and 3D analyses is in agreement with previous data (Solari 1969, Richler *et al.* 1987). It might result from different properties of the X and Y chromosomes such as their DNA content, their amount of heterochromatin or their degree of homology to each other. The total DNA content of the SV does not seem to be important in this case, as human and mouse X and Y chromosomes are very similar, with about 165 Mb for the X and 60 Mb for the Y (Morton 1991, Bishop 1992). The lack of heterochromatin on the mouse Y chromosome does not seem to be responsible for the undercondensation of the mouse SV as no difference was detected between human and chimpanzee SVs. The sequence homology between differentiated regions of the X and Y chromosomes is extremely reduced in mouse (Mitchell 2000), in contrast to the situation in human and chimpanzee. This characteristic of the mouse sex chromosomes could be sufficient to prevent the occurrence of damaging recombination events and make SV condensation unnecessary. Therefore, different mechanisms may be involved in the formation of the mammalian SV. In human and chimpanzee, the mechanism initiating SV formation may involve a precocious and rapid condensation of the sex chromosomes beginning zygonema, to prevent accidental recombination events between sex chromosomes and autosomes, and between X and Y differentiated regions. In mice, it may only involve a precocious isolation of the sex chromosomes from the autosomal bivalents. This separation is apparent as a clear space that becomes visible around the chromatin from the zygotene stage (Solari 1969).

Whatever its origin, differences in condensation of the human and mouse SVs suggest that X and Y chromosome condensation is not a prerequisite for the formation of the SV, which casts doubt on the role of XIST/Xist in this process. It is generally assumed that the condensation and the subsequent inactivation of the chromatin in the SV result from the same mechanism as X-chromatin inactivation in female mitotic cells (Richler *et al.* 1992, Salido *et al.* 1992, Armstrong *et al.* 1994, Ayoub *et al.* 1997). However, XIST/Xist gene expression is detectable from the spermatogonial stage (McCarrey & Dilworth 1992), which does not correspond to the stage at which the SV is formed. In addition, the Xist expression level is lower in adult mouse testes than in female somatic tissues, and the presence of transcripts in the testis can only be detected using PCR or PCR *in situ* (Salido *et al.* 1992, Ayoub *et al.* 1997). Such an observation is difficult to reconcile with a role for XIST in SV condensation, especially since X and Y chromosomes are both inactivated in the SV. Another argument against a role for the XIST/Xist gene in SV formation is that Xist knock-out did not result in male infertility in the mouse (Marahrens *et al.* 1997). All these discrepancies suggest that the SV formation is not a consequence of XIST/Xist expression. Therefore, the low level of XIST/Xist expression detected in the SV may only represent a basal transcription, resulting from the whole genome demethylation that occurs in the spermatogonia (Ariel *et al.* 1995), and similar to the 'pin point' transcription detected by FISH in XX and XY undifferentiated embryonic cells (Lee & Jaenisch 1997).

Differences in condensation of the human and mouse SVs could be related to different protein composition. To our knowledge, no human protein and only a few mouse proteins have been described as specific to the sex vesicle (Smith & Benavente 1992, Kralewski *et al.* 1997, Motzkus *et al.* 1999), but little is known about their precise functions. Two mechanisms might be involved in the SV condensation. The first, present at zygonema in human and chimpanzee, would be necessary to prevent XY exchanges between dispersed homologous sequences. This mechanism would not be required in mouse. The second mechanism, acting at late pachynema and easily observable in mouse, would be required to condense any unpaired segment before the first meiotic division. Indeed, condensation of chromo-

somes is essential for their accurate segregation during the cell cycle (Koshland & Strunnikov, 1996). In support of this hypothesis, the mouse $M31^{p21}$ protein, nuclear isoform of HP1 (Motzkus *et al.* 1999), was shown to localize to the SV only from mid-pachynema, in agreement with the variation of the sex chromatin condensation in mouse.

Our comparative analysis of human, chimpanzee and mouse pachytene nuclei highlights some important processes involved in the formation of the sex vesicle. The precocious condensation of the sex chromosomes is not required for the initiation of the mouse SV, as condensation only takes place at late pachynema. The organization and condensation of the sex chromosomes into two separate domains, and the clustering of their telomeres, might be essential processes in the formation of the SV, since they are features common to all three species.

Acknowledgements

We are grateful to Dr. J. Lorca and Professor C. Richaud for providing the patient material. We wish to thank Dr. A. Massacrier for her help in preparing the testis cryosections, Dr. M. Mitchell and Professor J. M. Luciani for their critical review of the manuscript. This work was supported by grants from INSERM, ARC (Association pour la Recherche contre le Cancer) and FRM (Fondation pour la Recherche Médicale).

References

Ariel M, Robinson E, McCarrey JR, Cedar H (1995) Gamete-specific methylation correlates with imprinting of the murine Xist gene. *Nat Genet* **9**: 312–315.

Armstrong SJ, Kirkham AJ, Hultén MA (1994) XY chromosome behaviour in the germ line of the human male: a FISH analysis of spatial orientation, chromatin condensation and pairing. *Chromosome Res* **2**: 445–452.

Ayoub N, Richler C, Wahrman J (1997) Xist RNA is associated with the transcriptionally inactive XY body in mammalian male meiosis. *Chromosoma* **106**: 1–10.

Bishop CE (1992) The mouse Y chromosome. *Mamm Genome* **3 Spec No**: S289–S293.

Bonhomme F, Guénet JL (1989) The wild mouse and its relative. In Lyon MF, Searle AG, eds., *Genetic Variants and Strains of the Laboratory Mouse*, 2nd edn. Oxford: Oxford University Press, pp 649–662.

Burgoyne PS (1982) Genetic homology and crossing over in the X and Y chromosomes of mammals. *Hum Genet* **61**: 85–90.

Chandley AC, Goetz P, Hargreave TB, Joseph AM, Speed RM (1984) On the nature and extent of XY pairing at meiotic prophase in man. *Cytogenet Cell Genet* **38**: 241–247.

Disteche CM, Tantravahi U, Gandy S, Eisenhard M, Adler D, Kunkel LM (1985) Isolation and characterization of two repetitive DNA fragments located near the centromere of the mouse X chromosome. *Cytogenet Cell Genet* **39**: 262–268.

Graves JAM, Wakefield MJ, Toder R (1998) The origin and evolution of the pseudoautosomal regions of human sex chromosomes. *Hum Mol Genet* **7**: 1991–1996.

Heard E, Mongelard F, Arnaud D, Avner P (1999) Xist yeast artificial chromosome transgenes function as X-inactivation centers only in multicopy arrays and not as single copies. *Mol Cell Biol* **19**: 3156–3166.

Koshland D, Strunnikov A (1996) Mitotic chromosome condensation. *Annu Rev Cell Dev Biol* **12**: 305–3333.

Kralewski M, Novello A, Bennavente R (1997) A novel Mr 77,000 protein of the XY body of mammalian spermatocytes: its localization in normal animals and in Searle's translocation carriers. *Chromosoma* **106**: 160–167.

Kvalov K, Galvagni F, Brown WRA (1994) The sequence organization of the long arm pseudoautosomal region of the human sex chromosomes. *Hum Mol Genet* **3**: 771–778.

Lansdorp PM, Verwoerd NP, van de Rijke FM *et al.* (1996) Heterogeneity in telomere length of human chromosomes. *Hum Mol Genet* **5**: 685–691.

Lee JT, Jaenisch R (1997) The epigenetic control of mammalian X-chromosome. *Curr Opin Genet Dev* **7**: 274–280.

Lengauer C, Green ED, Cremer T (1992) Fluorescence in situ hybridization of YAC clones after alu-PCR amplification. *Genomics* **13**: 826–828.

Luciani JM, Morazzani MR, Stahl A (1975) Identification of pachytene bivalents in human male meiosis using G-banding technique. *Chromosoma* **52**: 275–282.

McCarrey J, Dilworth DD (1992) Expression of Xist in mouse germ cells correlates with X-chromosome inactivation. *Nat Genet* **2**: 200–203.

McKee BD, Handel MA (1993) Sex chromosomes, recombination, and chromatin conformation. *Chromosoma* **102**: 71–80.

Marahrens Y, Panning B, Dausman J, Strauss W, Jaenisch R (1997) Xist-deficient mice are defective in dosage compensation but not spermatogenesis. *Genes Devel* **11**: 156–166.

Metzler-Guillemain C, Mignon C, Depetris D, Guichaoua MR, Mattei MG (1999) Bivalent 15 regularly associates with the sex vesicle in normal male meiosis. *Chromosome Res* **7**: 369–378.

Mitchell MJ (2000) Spermatogenesis and the mouse Y chromosome: specialisation out of decay. In: *Results and Problems in Cell Differentiation*. Berlin Heidelberg: Springer-Verlag, p 28.

Morton NE (1991) Parameters of the human genome. *Proc Natl Acad Sci USA* **88**: 7474–7476.

Motzkus D, Singh PB, Hoyer-Fender S (1999) M31, a murine homolog of drosophila HP1, is concentrated in the XY body during spermatogenesis. *Cytogenet Cell Genet* **86**: 83–88.

Parazza F, Humbert C, Usson Y (1993) Method for 3D volumetric analysis of intranuclear fluorescence distribution in confocal microscopy. *Comput Med Imag Graph* **17**: 189–200.

Parazza F, Bertin E, Wozniak Z, Usson Y (1995) Analysis of the spatial distribution of the AgNOR proteins in cell nuclei using simultaneous confocal scanning laser fluorescence and transmitted light microscopy. *J Microsc* **178**: 251–260.

Parraga M, Del Mazo J (2000) XYbp, a novel RING-finger protein, is a component of the XY body of spermatocytes and centrosomes. *Mech Dev* **90**: 95–101.

Pinkel D, Straume T, Gray JW (1986) Cytogenetic analysis using quantitative, high sensitivity, fluorescence hybridization. *Proc Natl Acad Sci USA* **83**: 2934–2938.

Popp S, Scholl HP, Loos P *et al*. (1990) Distribution of chromosome 18 and X centric heterochromatin in the interphase nucleus of cultured human cells. *Exp Cell Res* **189**: 1–12.

Rettenberger G, Zimmermann W, Klett C, Zechner U, Hameister H (1995) Mapping of murine YACs containing the genes Cea2 and Cea4 after B1-PCR amplification and FISH analysis. *Chromosome Res* **3**: 473–478.

Richler C, Soreq H, Wahrman J (1992) X inactivation in mammalian testis is correlated with inactive X-specific transcription. *Nat Genet* **2**: 192–195.

Richler C, Uliel E, Kerem BS, Wahrman J (1987) Regions of active chromatin conformation in "inactive" male meiotic sex chromosomes in the mouse. *Chromosoma* **95**: 167–170.

Salido EC, Yen PH, Mohandas TK, Shapiro LJ (1992) Expression of the X-inactivation-associated gene Xist during spermatogenesis. *Nat Genet* **2**: 196–199.

Salido EC, Li XM, Yen PH, Martin N, Mohandas TK, Shapiro LJ (1996) Cloning and expression of the mouse pseudoautosomal steroid sulphatase gene (Sts). *Nat Genet* **13**: 83–86.

Schmid M, Haaf T (1984) DistamycinA/DAPI bands and the effects of 5-azacytine on the chromosomes of the chimpanzee, *Pan troglodytes. Cytogenet Cell Genet* **38**: 192–199.

Schnedl W, Dev VG, Trantravahi R, Miller DA, Erlanger BF, Miller OJ (1975) 5-Methylcytosine in heterochromatic regions of chromosomes: chimpanzee and gorilla compared to human. *Chromosoma* **52**: 59–66.

Sharp P (1982) Sex chromosome pairing during male meiosis in marsupials. *Chromosoma* **86**: 27–42.

Sherthan H, Weich S, Schwegler H, Heyting C, Härle M, Cremer T (1996) Centromere and telomere movements during early meiotic prophase of mouse and man are associated with the onset of chromosome pairing. *J Cell Biol* **134**: 1109–1125.

Smith A, Benavente R (1992) Meiosis-specific protein selectively associated with sex chromosomes of rat pachytene spermatocytes. *Proc Natl Acad Sci USA* **89**: 6938–6942.

Solari AJ (1969). The evolution of the ultrastructure of the sex chromosomes (sex vesicle) during meiotic prophase in mouse spermatocytes. *J Ultrastruct Res* **27**: 289–305.

Solari AJ (1974) The behaviour of the XY pair in mammals. *Int Rev Cytol* **38**: 273–317.

Solari AJ (1980) Synaptonemal complexes and associated structures in microspread human spermatocytes. *Chromosoma* **81**: 315–337

Solari AJ (1989) Sex chromosome pairing and fertility in the heterogametic sex of mammals and birds. In: Gillies CB, ed. *Fertility and Chromosome Pairing. Recent Studies in Plants and Animals*. Boca Raton, Florida: CRC Press, pp 77–107.